Twenty-Seventh Symposium (International) on Combustion/The Combustion Institute, 1998/pp. 633–640

MEASUREMENTS OF FORMALDEHYDE CONCENTRATIONS AND FORMATION RATES IN A METHANE-AIR, NON-PREMIXED FLAME AND THEIR IMPLICATIONS FOR HEAT-RELEASE RATE

MICHAEL P. TOLOCKA AND J. HOUSTON MILLER
Department of Chemistry
The George Washington University
Washington, DC 20052, USA

Tunable diode laser absorption spectroscopy coupled with microprobe sampling was used to quantitatively determine formaldehyde concentrations in a methane-air non-premixed flame. Resulting concentration profiles are similar in shape and peak locations to previous qualitative measurements, and concentration levels are in line with those predicted by direct numerical simulation of methane-air flames. The resulting concentrations were combined with other data from this flame system in a mixture fraction-based code to predict levels for species whose concentrations are not available experimentally. An analysis was performed of formaldehyde formation and destruction paths to determine HCHO's dependence on specific reaction steps. Formaldehyde formation is dominated by the reaction between methyl radical and oxygen atom, and it is destroyed by hydrogen abstraction. Both processes occur near the stoichiometric surface. The analysis also verified several points made by other researchers about the heat-release rates in methane flames. Heat-release rate correlates well with the destruction rate of methane, the rate of the reaction between methyl radicals and oxygen atoms, and HCO· concentrations. A condition of chemical steady state is found for HCO·, and the steady-state estimate of HCO· concentration may also be used to estimate local heat-release rate in methane flames.

Introduction

In the Navier Stokes treatment of combustion, energy and mass conservation requires simultaneous solution of individual equations for each of the chemical species in the system. For turbulent flames, the computational costs of including full chemistry is prohibitive. For non-premixed flames, conserved scalar conservation has been used as a surrogate for the individual species mass conservation equations. By definition, conserved scalars have no source terms, and these new mass conservation equations require only treatment of convection and diffusion. However, even within the conserved scalar model, energy conservation is more complex in that some treatment of the source term, that is, heat-release rate, is still required.

There has been a considerable body of experimental work aimed at characterizing the heat-release region of both premixed and non-premixed flames [1]. This work has been reviewed by Najm et al. in a recent paper [2]. Most of these measurements have utilized optical diagnostics, and they include both chemiluminescence of nascent species (CH^*, CO_2^*, C_2^*, and OH^*) as well as laser-induced fluorescence measurements of radicals such as CH· and OH·. Because significant measurement interferences exist when polynuclear aromatic hydrocarbons and soot are present, many of these measurements have been performed in diluted flames. Thus, the application of the results to neat flames is problematic.

In the Najm et al. work [2], LIF measurements of the HCO· radical show that its concentration spatially and temporally correlates with local heat release. Unfortunately, signals are sufficiently weak that planar imaging measurements of the fluorescence do not provide adequate signal-to-noise levels.

In a recent study of flickering flames, Kaplan et al. [3] developed a simple model for heat release that is derived from a conserved scalar treatment of fuel consumption [4]. In Bilger's work [4], methane consumption in a steady flame can be calculated from

$$\dot{\omega}_{CH_4} = -\rho\, D\, (\nabla\xi)^2 \frac{\partial^2 Y_{CH_4}}{\partial \xi^2} \qquad (1)$$

where ρ is the mixture density, Y_{CH_4} is the mass fraction of methane, D is the mixture diffusion coefficient and ξ is the mixture fraction. In the Kaplan et al. [3] paper, five chemical species were tracked in the flow: CH_4, O_2, N_2, CO_2, and H_2O. Nitrogen was assumed to be chemically inert, and the other four species were linked through the global combustion reaction. Heat release was calculated by multiplying the fuel-consumption rate by the heat of combustion.

There seem to be two unsatisfactory aspects of the approach adopted by Kaplan et al. [3]. First, there

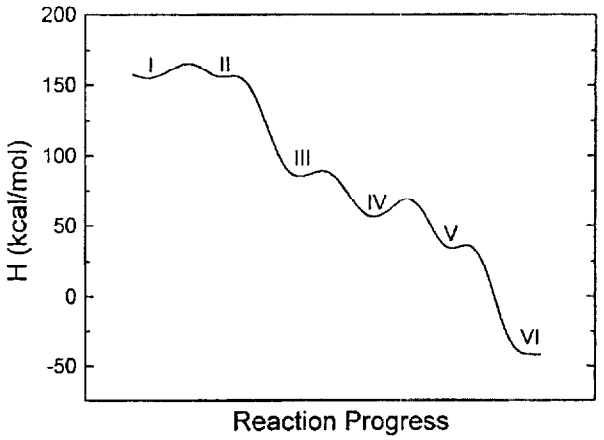

FIG. 1. Enthalpy flow along the reaction coordinate linking methane and carbon dioxide. In this simplified scheme, states (at 1900 K) are as follows: I: CH_4 + 2H· + O: + OH·; II: CH_3· + O: + H· + OH· + H_2; III: HCHO + 2H· + OH· + H_2; IV: HCO· + H· + OH· + $2H_2$; V: CO + H· + OH· + $2H_2$; and VI: CO_2 + H· + $2H_2$.

is little validation for how well it works. Second, because it assumes a single-step, irreversible chemical model, it does not provide much guidance for the advancement of diagnostics for heat release that have focused on intermediate species.

Between single-step and full treatments of chemical heat release is the use of a reduced chemical mechanism. Typically, one begins with a larger mechanism, culls slow processes, and uses steady-state and partial equilibrium assumptions to algebraically simplify the calculations of flame chemistry. For methane combustion, a variety of short mechanisms have been proposed. Peters and coworkers developed a four-step mechanism for methane combustion that has been applied to both premixed [5] and counterflow diffusion flames [6,7]. As noted by Bilger et al. [8], this reduced mechanism overpredicts the strain rate at extinction and does not provide good estimates for radical species on the fuel-rich side of the high-temperature reaction zone in diffusion flames. In the latter work [8], the authors develop a four-step mechanism that corrects these deficiencies by re-examining partial equilibrium and steady-state assumptions made in the Peters references. Common to both mechanisms is the irreversible fuel consumption reaction:

$$CH_4 + 2H\cdot + H_2O \rightarrow CO + 4H_2 \quad \text{(R1)}$$

In reduced mechanisms, the rates of the consolidated steps are derived from rates of elementary reaction processes. In the work of Bilger et al. [8], the main reaction path leading from methane to carbon dioxide was shown to be

$$CH_4 + H\cdot \rightleftharpoons CH_3\cdot + H_2 \quad \text{(R2)}$$

$$CH_3\cdot + O: \rightleftharpoons HCHO + H\cdot \quad \text{(R3)}$$

$$HCHO + H\cdot \rightleftharpoons HCO\cdot + H_2 \quad \text{(R4)}$$

$$HCO\cdot + M \rightleftharpoons H\cdot + CO + M \quad \text{(R5)}$$

$$CO + OH\cdot \rightleftharpoons CO_2 + H\cdot \quad \text{(R6)}$$

Figure 1 follows the flow of energy along this reaction path. Despite the fact that stable carbon-containing molecules (i.e., HCHO and CO) exist along the path, all of these elementary steps are exothermic and largely irreversible. Further, in the Bilger et al. analysis [8], all of the carbon intermediates between fuel and carbon dioxide with the exception of CO are found to be in chemical steady state. Using these steady-state relationships, the authors were able to show that the rate of fuel consumption, reaction R1, is given by the sum of four elementary reactions that produce formaldehyde, dominated by R3: the reaction of methyl and oxygen atoms. Further, the steady-state expression for the concentration of the formyl radical presented in Ref. [8] is also a linear function of formaldehyde formation rates.

To briefly summarize the discussion so far, in methane flames, the fuel-consumption rate, which should be a good surrogate for heat-release rate, is determined by formaldehyde formation rates that also establish the steady-state concentration for the HCO· radical. Thus, a link may be established between the experimental work of Najm et al. [2], the heat-release model of Kaplan et al. [3], and the reduced mechanisms that preceded both. Central to this picture is formaldehyde chemistry.

Calculations [9] of formaldehyde concentrations in methane-air flames indicate that peak concentrations should be near 1 part per thousand. However, formaldehyde concentrations have been found to be as much as a few percent in flames with high strain rates [6], a fact which may have implications for turbulent flames where simplified reduced mechanisms may fail to accurately predict formaldehyde levels [10].

Previous attempts of measuring formaldehyde in flames have met with some obstacles. Gas chromatographic measurements [11] require long sampling and analysis times. Also, storage of the gases can lead to sample degradation through oxidation of formaldehyde to formic acid. Although the visible spectroscopic parameters such as line widths and absorption cross sections for HCHO are well known [12,13], quantitative LIF measurements suffer from interferences from broadband PAH fluorescence. Furthermore, partition function effects decrease signal intensity at higher temperatures [14]. Mass spectrometric measurements are hampered by isobaricity of other combustion intermediates at 30 amu, such as ethane. Mass spectrometry also requires calibration to accurately obtain quantitative information [15].

Over the past several years, a substantial body of data has been collected on the structure of a

methane-air flame supported on a Wolfhard Parker slot burner. Concentrations for all of the major flame species, as well as many minor ones, have been determined. Because of this wealth of information, this flame system provides an ideal environment to test ideas on heat release. In this paper, we present measurements of formaldehyde concentration using tunable diode laser absorption spectroscopy (TDLAS). In our lab, we have demonstrated the use of TDLAS as an effective diagnostic of many small molecules in flames such as CO, CO_2 [16], CH_4, C_2H_2 [17], and NO· [18]. Previous measurements of formaldehyde line strengths [19] and broadening parameters [20] have been determined in order to develop the technique for measurements in flames and the atmosphere [21–23]. It should be noted that low concentrations coupled with relatively low line strengths (on the order of 10^{-21} $cm^{-1}/(cm^{-2}$ molecules) lead to low signal levels for *in situ* flame measurements. For that reason, in the work presented here, we couple extractive microprobe sampling with 2*f* wavelength modulation spectroscopy (WMS) [24–26] to give the detection limits and sensitivity required. Measured concentrations are combined with previously determined data to analyze formaldehyde formation and destruction pathways. Finally, an analysis of heat-release rates in this system tests the importance of formaldehyde formation in predicting methane consumption rates, heat-release rates, and HCO· concentrations.

Experimental Determination of Formaldehyde

The burner consists of a central rectangular fuel slot with dimensions of 8 × 40 mm sandwiched between two adjacent air slots with dimensions of 16 × 40 mm. Wire screen gulls were used to stabilize the 300-mm flame. A quartz microprobe with an orifice diameter of 140 μm was inserted along the longitudinal axis of the flame at select heights above the burner (HAB) surface. The burner was moved underneath the microprobe in order to collect spectra at different lateral and longitudinal positions. The spectra were collected every 0.2 mm from −10 to 10 mm laterally. The microprobe withdrew the combustion gases into a 2025-cm path-length White cell. The pressure in the cell was monitored by a capacitance manometer and was kept at ~ 20 Torr by throttling a valve before the gases were drawn into a rotary pump. Operating at low pressure minimized overlap from neighboring methane lines. It should be noted that in the wavelength of interest, the methane line just to the blue of the formaldehyde absorption (discussed later) would obscure the formaldehyde signal at atmospheric pressure. Good agreement has been found between shapes of species' profiles and peak locations with extractive and *in situ* techniques in this burner system [27,28].

Light from a diode laser operating at 2936 cm^{-1} was collimated and passed through a monochromator to select a single laser mode. Fine tuning the diode laser by changing the current allowed for the scanning of the absorption features. To perform wavelength modulation spectroscopy (WMS), the current applied to the laser was modulated at 8.9 kHz, as it was scanned through an absorption feature. The emitted laser light was chopped at 401 Hz using a tuning fork chopper for the discrimination of laser radiation from the background radiation. The light was directed around the optical table and through the long path absorption cell using reflective optics. The resulting attenuated radiation was collected on a parabolic mirror and focussed onto a liquid nitrogen–cooled InSb detector. The signal from this detector was split to the two lock-in amplifiers. The chopper was referenced to the first lock-in amplifier to determine I^0. The high-frequency modulation was used to reference another phase-sensitive, digital lock-in amplifier for the collection of x'' as described previously [16–18]. The signal x'' is related to the analyte concentration through [25]

$$x'' = F_2 \times S(T) \times g(\nu^0) \times P_j \times L \times I^0 \quad (2)$$

where F_2 is the second Fourier component of the modulation signal, $S(T)$ is the line strength as function of temperature, g is the line-shape factor, P_j is the partial pressure of the absorbing gas, L is the path length, and I^0 is the incident signal. This technique is well known for increasing the detection limits for a given analyte [23,25].

The HCHO concentrations were determined by fitting the 2*f* spectra using a PASCAL program described previously [16,17]. The parameters in the fitting routine included the concentration of the analyte as well as an adjacent H_2O absorption. As shown in the spectrum in Fig. 2, the HCHO absorption ($17_{4,14} \leftarrow 16_{3,13}$ of the ν_5 fundamental) lies quite close to a rather large methane absorption (*P*(8) *F*2(2) of the ν_3 band [29]). Methane levels were fixed to concentrations established previously [30]. Adding the methane concentration as a parameter of the fitting procedure did not have a significant effect on the resulting concentrations. Another important feature of the spectrum lies just red of the formaldehyde absorption. This absorption was not found in the HITRAN [31] database. Fits were performed to establish the concentration of the unknown species responsible for this absorption. However, the quality of the fits in the vicinity of the formaldehyde were worse than if the absorption was ignored, and this latter approach was adopted for the results subsequently presented.

Formaldehyde Concentrations

The results of the measurements at 3, 5, 7, 9 and 11 mm HAB are shown in Fig. 3. The maximum

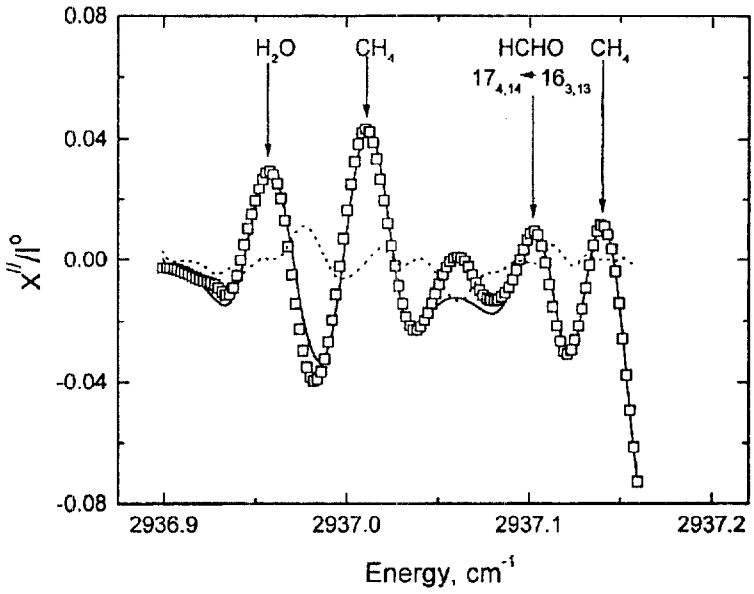

FIG. 2. Spectrum of formaldehyde in flame gases taken at 9 mm HAB 2 mm off of the burner centerline. Open symbols indicate experimental data, the solid line indicates the fit to the data, and the broken line is the residual of the fitting process (described in text).

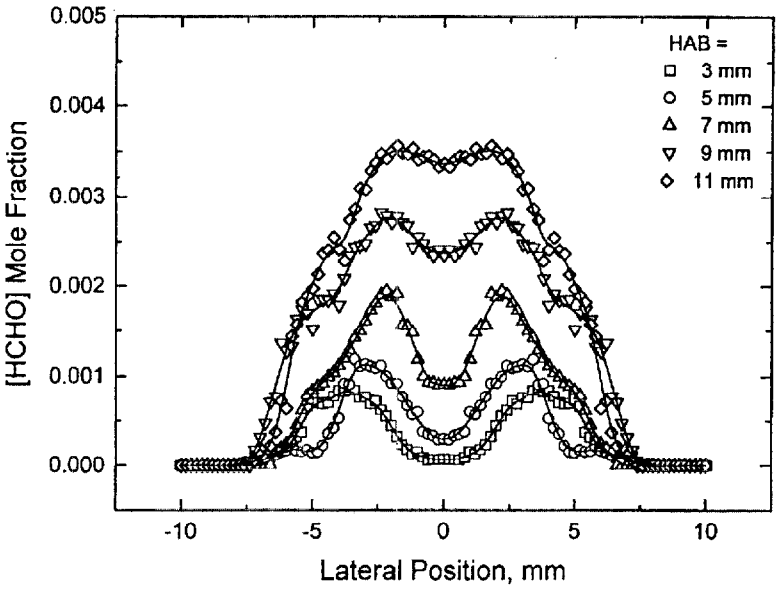

FIG. 3. Concentrations of formaldehyde in the Wolfhard–Parker diffusion flame at several heights above the burner (HAB). □: 3 mm HAB; O: 5 mm HAB; Δ: 7 mm HAB; ∇: 9 mm HAB; and ◇: 11 mm HAB.

concentration is observed to be about 3.2 parts per thousand at 11 mm HAB at a lateral position of 2 mm off of the burner centerline, a location substantially rich of the stoichiometric surface (which lies at 6.5 mm at this height). These concentration levels are in good agreement with model predictions of formaldehyde in methane-air diffusion flames. Further, the profiles appear to be similar in shape to those obtained by Harrington and Smyth [14]. The observed growth of the profiles toward the burner centerline is clearly evident as the maximum concentration changes from a lateral location of 3.5 to 2 mm from the centerline from 3 to 11 mm HAB, respectively. Similar trends in hydrocarbon profiles have been ascribed to chemical production near the stoichiometric surface followed by convection and diffusion toward the flame interior [32].

Reaction Path Analysis

As noted in the Introduction, the data available in the Wolfhard–Parker (WP) flame provide an opportunity to examine formaldehyde chemistry in some detail. Even so, there are many species that are important in methane oxidation whose concentrations are unknown in this flame. For example, Smooke has applied a 26-species mechanism to the determination of methane-air flame structure that includes both one-carbon and two-carbon species but no nitrogen oxidation. Of these 26 species, only 14 are available in the WP flame from experimental measurements (specifically, HCHO as well as CH_4, O_2, N_2, CO_2, H_2O, CO, H_2, C_2H_2, OH·, H atom, O atom, and CH_3·, and CH· [9,27,32–35]). To estimate the concentrations of the remaining species, we have adopted the computational scheme described later.

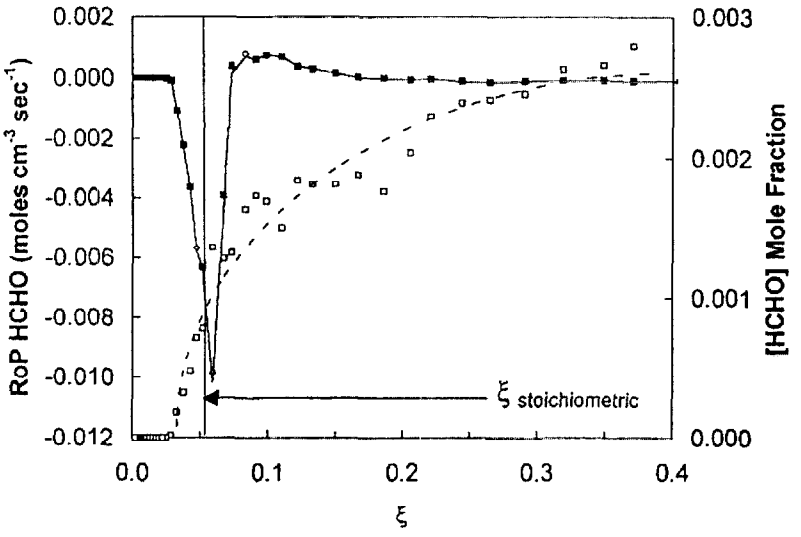

FIG. 4. Rate of production analysis of formaldehyde chemistry in the WP flame at 9 mm HAB. □ is the concentration of HCHO as a function of ξ, with the dashed line through the data used to illustrate the trend. ■ indicates the ROP of HCHO as a function of mixture fraction, ξ. O indicates flame location of maximum production rate at ξ = 0.0829, Δ represents the maximum destruction rate at ξ = 0.0589, and ◇ is at ξ = 0.0474. These points are where the sensitivity analysis was performed. Solid line shows the calculation of the ROP from only the four reactions shown in Fig. 5.

It has been well established that conserved scalars such as mixture fraction can be used to correlate many combustion species' concentrations [4,36]. An implication of this observation is that the species conservation equations may be rewritten as a function of mixture fraction:

$$\frac{d(\rho Y_i)}{dt} = \dot{\omega}_i - \frac{\rho\chi}{2}\frac{\partial^2 Y_i}{\partial\xi^2} \qquad (3)$$

where t, ω, ρ, ξ, χ, and Y_i are time, chemical rate (in grams per cc per second), mixture mass density, mixture fraction, scalar dissipation rate, and the mass fraction of species i, respectively. Both ξ and χ have been previously computed for the WP data.

In a steady flame, the left-hand side of equation 3 should be zero for all species. The code minimized the difference between the two terms on the right-hand side of the equation for all chemical species in the mechanism by iterating the mass fractions of only the experimentally undetermined species using a implicit time step of 100 ns. Convergence was achieved after 25 ms as determined through several tests in which mole fractions of all species were found to change less than 0.1% per time step. Although initial calculations were done with a Smooke mechanism [9,37] which contained 26 species and 83 reactions, the results presented here were obtained using GRI Mech 1.2 [38]. Finally, linear boundary conditions were imposed at ξ = 0 (pure air at 298 K) and ξ = 1 (pure methane at 298 K).

At the conclusion of the calculations, concentrations and rates of production (ROP) for all the species were reported and sensitivity coefficients [39] for selected species were computed. The resulting ROP for formaldehyde versus mixture fraction is shown in Fig. 4. Also shown in the figure is the mole fraction of formaldehyde at 9-mm HAB plotted against mixture fraction. An important observation in this figure is the disparity between the location of the maximum in the formaldehyde concentration (ξ = 0.4) and its dominant production rate features, which occur near the stoichiometric surface. Note that the ROP profile consists of two features: a destruction feature at the stoichiometric surface and a smaller production feature on the rich side. As formaldehyde is formed, it will diffuse to both richer and leaner stoichiometries. Molecules that diffuse to leaner stoichiometries are destroyed. However, diffusion to richer stoichiometries carries HCHO into the chemically inert flame interior where its concentration grow.

Figure 5 shows sensitivity coefficients calculated for formaldehyde at three stoichiometries: near the stoichiometric surface (ξ = 0.0589), slightly rich (ξ = 0.0830), and slightly lean (ξ = 0.0470). The resulting chemistry appears to be quite simple. There are two major formation pathways for formaldehyde: methyl attack by oxygen atom and methyl attack by the hydroxyl radical, with the former being substantially more important (about 75%). Formaldehyde destruction is entirely through hydrogen abstraction by H atom, O atom, and OH· with the relative dominance of each pathway shifting with stoichiometry.

Heat-Release Rate Correlations

The heat-release rate as a function of mixture fraction can be determined by summing the products of net chemical formation rates $\dot{\omega}_i$ and specific enthalpies h_i for all species i:

$$\dot{Q} = \sum_i \dot{\omega}_i h_i \qquad (4)$$

As a first test, the heat-release rate $\dot{Q}$ was plotted against methane destruction rates and a reasonable linear correlation was obtained (r^2 = 0.9211) with a slope of −136 kJ/mol, substantially less than the heat of combustion of methane (−890 kJ/mol). In the work of Najm et al. [2], correlations of heat release showed a similar "petal" appearance with a rich

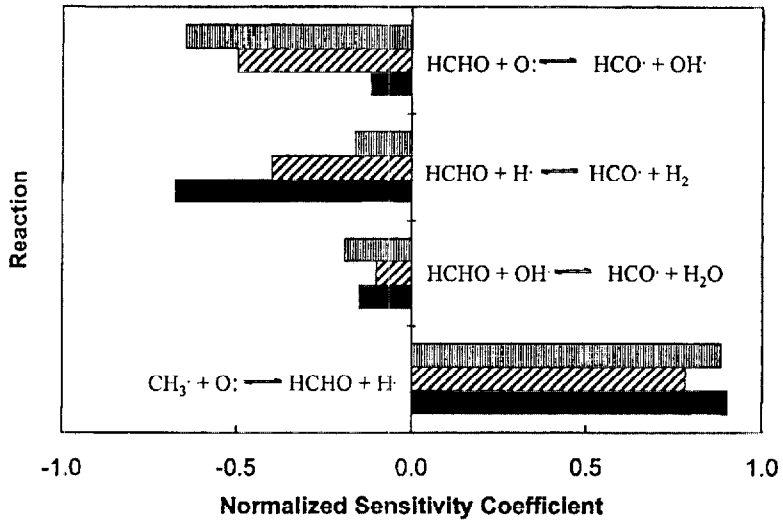

FIG. 5. Normalized sensitivity coefficients for formaldehyde as a function of location in the flame. Gray, striped, and black bars are the sensitivity coefficients lean of, at, and rich of the stoichiometric surface, respectively. (See text for details.)

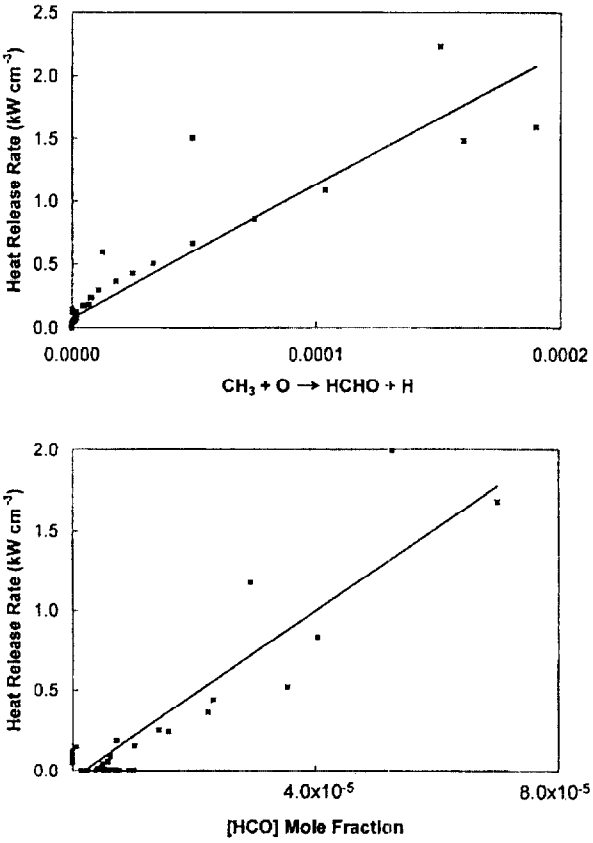

FIG. 6. (A) Heat-release rate (kW cm^{-3}) plotted against rate of the forward reaction $CH_3\cdot + O: \rightleftharpoons HCHO + H\cdot$ (moles cm^{-3} sec^{-1}). (B) Heat-release rate (kW cm^{-3}) versus formyl radical concentrations.

(lower) and lean (upper) branch. Obviously, consideration of only one of these branches improves the quality of the correlation.

The picture for formaldehyde chemistry revealed in our work is even simpler than the Bilger et al. [8] reduced scheme might have suggested. Here the dominant contribution to formaldehyde formation comes from the reaction of methyl and oxygen atom. Recall that Bilger et al. [8] predicted that the rate of methane destruction could be determined by the rate of formaldehyde formation. In that case, and in light of the successful correlation of the heat-release rate with the methane destruction rate, it would seem reasonable that the forward rate of the reaction between $CH_3\cdot$ and O atom would also correlate well with the heat-release rate. This correlation is shown in Fig. 6A. As expected, this correlation is also quite good ($r^2 = 0.8472$).

An additional prediction of the Bilger et al. [8] work is that if both HCHO and HCO· are in chemical steady state HCO· concentrations should be linear functions of formaldehyde formation rates. Therefore, formyl radical concentrations should also correlate with the heat-release rate. This correlation is shown in Fig. 6B. Finally, our analysis shows that the simplicity of formaldehyde chemistry is mirrored in that of HCO·. Formyl is formed through hydrogen atom abstraction from formaldehyde and destroyed through thermal decomposition. Further, HCO· appears to be in steady state: The peak in the formyl radical ROP profile is substantially smaller than the rates of the dominant individual reactions that form and destroy it. Thus, HCO· may be estimated from

$$[\mathrm{HCO}] = \frac{[\mathrm{HCHO}]\,(k_6[\mathrm{O}] + k_7\,[\mathrm{OH}] + k_3\,[\mathrm{H}])}{k_4[\mathrm{M}]} \qquad (5)$$

Although this steady-state estimate overpredicts the HCO· concentration calculated in our one-dimensional code by a factor of 3, the peak location and peak shape (in mixture fraction space) are well predicted. Thus, the steady-state estimate of HCO· may also be used to correlate heat-release rates. This result has implications for experimental systems in

which the measurement of formaldehyde is more accessible than that of the formyl radical.

Conclusions

Tunable diode laser absorption spectroscopy coupled with microprobe sampling has been used to quantitatively determine formaldehyde concentrations in a well-characterized methane-air non-premixed flame. Resulting concentration profiles are similar in shape and peak locations to previous qualitative measurements, and concentration levels are in line with those predicted by direct numerical simulation of methane-air flames. The resulting concentrations were combined with other data from this flame system in a mixture fraction-based code to predict levels for species whose concentrations are not available experimentally. Finally, an analysis was performed of formaldehyde formation and destruction reaction paths to determine HCHO's dependence on specific reaction steps.

Formaldehyde formation is dominated by the reaction between methyl radical and oxygen atom, and it is destroyed by hydrogen abstraction. Both processes occur near the stoichiometric surface. The analysis also verified several points made by other researchers about the local heat-release rate in methane flames:

- First, the heat-release rate correlates well with the destruction rate of methane.
- Second, because the latter may be determined by the formation rate of formaldehyde, the reaction rate of methyl radicals and oxygen atoms also may be used to predict heat-release rates.
- Finally, formyl radical concentrations, which are also dependent on formaldehyde formation rates, correlate well with heat-release rate. Moreover, a condition of chemical steady state is found for HCO· in our analysis, and the steady-state estimate of HCO· concentration may be used to estimate heat-release rate in methane flames.

Acknowledgments

The authors would like to thank the National Institutes of Standards and Technology (NIST) and the National Science Foundation for their generous financial support. The authors would also like to thank P. H. Paul for providing to us a prepublication manuscript.

REFERENCES

1. Clemens, N. T. and Paul, P. H., *Combust. Flame* 102:271–284 (1995).
2. Najm, H. N., Paul, P. H., Meuller, C. J., and Wyckoff, P. S., *Combust. Flame* 113:312–332 (1998).
3. Kaplan, C. R., Shaddix, C. R., and Smyth, K. C., *Combust. Flame* 106:392–405 (1996).
4. Bilger, R. W., *Combust. Sci. Technol.* 13:155–170 (1976).
5. Peters, N., in *Numerical Simulation of Combustion Phenomena* (R. Glowinski, B. Larrouturou, and R. Temam, eds.), Lecture Notes in Physics 241, Springer-Verlag, Berlin, 1985, pp. 90–109.
6. Peters, N. and Kee, R. J., *Combust. Flame* 68:17–30 (1987).
7. Seshadri, K. and Peters, N., *Combust. Flame* 73:23–44 (1988).
8. Bilger, R. W., Stårner, S. H., and Kee, R. J., *Combust. Flame* 80:135–149 (1990).
9. Norton, T. S., Smyth, K. C., Miller, J. H., and Smooke, M. D., *Combust. Sci. Technol.* 90:1–34 (1993).
10. Chen, J. Y. and Dibble, R. W., in *Reduced Kinetic Mechanisms and Asymptotic Approximations for Methane-Air Flames* (M. D. Smooke, ed.), Springer-Verlag, New York, 1991, p. 193.
11. Peeters, J. and Mahnen, G., in *Fourteenth Symposium (International) on Combustion*, The Combustion Institute, Pittsburgh, 1973, p. 773.
12. Cantrell, C. A., Davidson, J. A., McDaniel, A. H., Shetter, R. E., and Calvert, J. G., *J. Phys. Chem.* 94:3902–3908 (1990).
13. Rogers, J. D., *J. Phys. Chem.* 94:4011–4015 (1990).
14. Harrington, J. and Smyth, K. C., *Chem. Phys. Lett.* 202:196–202 (1993).
15. McKinnon, J. T., Ph.D. thesis, Massachusetts Institute of Technology, 1989.
16. Skaggs, R. R., Ph.D. thesis, The George Washington University, Washington, D.C., 1997.
17. Tolocka, M. P. and Miller, J. H., *Microchem. J.* 50:399–426 (1994).
18. Hill, D., Marro, M., and Miller, J. H., unpublished results.
19. Nadler, S., Daunt, S. J., and Reuter, D. C., *Appl. Opt.* 26:1641–1646 (1987).
20. Cline, D. S. and Varghese, P. L., *Appl. Opt.* 27:3219–3224 (1988).
21. Mackay, G. L., Karecki, D. R., and Schiff, H. I., *J. Geophys. Res.* 101:14721–14728 (1996).
22. Fried, A., Sewell, B., Henry, B., Wert, B. P., Gilpin, T., and Drummond, J. R., *J. Geophys. Res.* 102:6253–6266 (1997).
23. Trapp, D. and deServes, C., *Atmospher. Environ.* 29:3239–3243 (1995).
24. Arndt, R., *Appl. Phys.* 36:2522–2524 (1965).
25. Reid, J. and Labrie, D., *Appl. Phys.* B26:203–210 (1981).
26. Skaggs, R. R. and Miller, J. H., in *Twenty-Sixth Symposium (International) on Combustion*, The Combustion Institute, Pittsburgh, 1996, p. 1181.
27. Miller, J. H. and Taylor, P. H., *Combust. Sci. Technol.* 52:139–145 (1987).
28. Smyth, K. C., *Combust. Sci. Technol.* 115:151–176 (1996).

29. Barnes, W. L., Susskind, J., Hunt, R. H., and Plyler, E. K., *J. Chem. Phys.* 56:5160–5172 (1972).
30. Wolfhard-Parker database, the National Institutes of Standards and Technology.
31. HITRAN database of infrared transition data, Air Force Geophysics Laboratory, 1996 ed.
32. Miller, J. H., Mallard, W. G., and Smyth, K. C., in *Twenty-First Symposium (International) on Combustion*, The Combustion Institute, Pittsburgh, 1986, p. 1057.
33. Smyth, K. C., Miller, J. H., Dorfman, R. C., Mallard, W. G., and Santoro, R. J., *Combust. Flame* 62:157–181 (1985).
34. Norton, T. S. and Smyth, K. C., *Combust. Sci. Technol.* 76:1–20 (1990).
35. Smyth, K. C. and Tjossem, P. J. H., in *Twenty-Third Symposium (International) on Combustion*, The Combustion Institute, Pittsburgh, 1990, p. 1829.
36. Marro, M. A. T., Ph.D. thesis, The George Washington University, Washington, D.C., 1997.
37. Puri, I. K., Seshadri, K., Smooke, M. D., and Keyes, D. E., *Combust. Sci. Technol.* 56:1 (1987).
38. Frenklach, M., Wang, H., Lu, C. L., Goldenberg, M., Bowman, C. T., Hanson, R. K., Davidson, D. F., Chang, E. J., Smith, G. P., Golden, D. M., Gardiner, W. C., Lissianski, V., http://www.me.berkeley.edu/gri_mech; and Frenklach, M., Wang, H., Goldenberg, M., Smith, G. P., Golden, D. M., Bowman, C. T., Hanson, R. K., Gardiner, W. C., and Lissianski, V., "GRI-Mech—An Optimized Detailed Chemical Reaction Mechanism for Methane Combustion," Gas Research Institute Topical report, report no. GRI-95-0058.
39. Kee, R. J., Rupley, F. M., and Miller, J. A., "CHEMKIN II: A Fortran Chemical Kinetics Package for the Analysis of Gas Phase Chemical Kinetics," Sandia report SAND89-8009B UC-706.